

Hydrophobic Mutagenesis and Semi-rational Engineering of Arginine Deiminase for Markedly Enhanced Stability and Catalytic Efficiency

Serwanja Jamil¹ · Meng-Han Liu¹ · Yong-Mei Liu¹ ·
Rui-Zhi Han¹ · Guo-Chao Xu¹ · Ye Ni¹

Received: 10 March 2015 / Accepted: 21 April 2015 /
Published online: 4 June 2015
© Springer Science+Business Media New York 2015

Abstract Due to its systemic arginine degradation, arginine deiminase (ADI) has attracted attentions as an anti-tumor drug. Its low activity at physiological conditions among other limitations has necessitated its engineering for improved properties. The present study describes the hydrophobic mutagenesis and semi-rational engineering of ADI from *Pseudomonas plecoglossicida* (PpADI). Using an improved ADI variant M13 (D38H/A128T/E296K/H404R/I410L) as parent, site saturation mutagenesis at position 162 resulted in an over 20 % increase in protein solubility. Compared with M13 (15.23 U/mg), mutants M13-2 (M13+S245D) and M13-5 (M13+R243L) exhibited enhanced specific activity of 21.19 and 31.20 U/mg at physiological conditions. M13-5 displayed enhanced substrate specificity with a dramatic reduction in its K_m value (from 0.52 to 0.16 mM). It is speculated that the improvements in M13-5 could mainly be attributed to the enhanced structural stability due to an R243L substitution. The hydrophobic contribution of Leu 243 was supported by mutant M13-9 (M13+A276W) generated based on the hydrophobic mutagenesis concept. M13-9 showed a specific activity of 18.68 U/mg, as well as remarkable thermal and pH stability. It retained over 90 % activity over pH range from 4.5 to 8.5. At 60 °C, the half-life of M13-9 was enhanced from 4 to 17.5 min in comparison with M13, and its specific activity at 62 °C (93.0 U/mg) was approximately fivefold of that determined at 37 °C. Our results suggest that the increased hydrophobicity around the active regions of PpADI might be crucial in improving its structural stability and ultimately catalytic efficiency.

Keywords Arginine deiminase · Protein engineering · Hydrophobic mutagenesis · Structural stability · Semi-rational engineering

✉ Ye Ni
yni@jiangnan.edu.cn

¹ The Key Laboratory of Industrial Biotechnology, Ministry of Education, Laboratory of Biocatalysis, School of Biotechnology, Jiangnan University, 1800 Lihu Rd., 214122 Wuxi, China

Introduction

Arginine deiminase (ADI, EC 3.5.3.6), an arginine-degrading enzyme, has recently attracted attention as a potential anti-tumor drug [1] due to its systemic arginine degradability in arginine auxotrophic tumors such as hepatocellular carcinomas (HCCs) and melanomas [2–5]. In addition, the enzyme also has a low mammalian toxicity and high substrate specificity and has been demonstrated to be well tolerated in patients with advanced melanomas and HCCs [6, 7]. Some reports even suggest that ADI could be a more potent drug against leukemia than L-asparaginase [4]. Due to its tremendous potential as an anti-tumor drug, clinical trials of ADI-PEG-20 against HCCs (phase III) [8] and melanomas [9] are underway. Previously, *Pseudomonas plecoglossicida* CGMCC2039 was isolated and identified for its high ADI activity [10]. However, one major limitation of *P. plecoglossicida* ADI (PpADI)'s utilization as an anti-tumor drug is its relatively low activity at physiological pH [1, 11]. Improvement of ADI's enzymatic properties by either directed evolution or structural-guided rational design has thus become necessary.

Directed evolution involves all protein engineering techniques such as error prone polymerase chain reaction (ep-PCR) and DNA shuffling which mimic the natural evolutionary process [12, 13]. Through such approaches, various properties of proteins have been improved [13–15]. However, due to certain limitations of directed evolutionary approaches [16, 17], some researchers have opted for structural-guided rational design [18]. Nevertheless, increasing reports seem to suggest that a combination of both approaches might be ideal in generating novel biocatalysts [19, 20], and as a result, a number of enzymes have been successfully engineered [21–24]. Recently, various enzymatic properties of PpADI have been improved by a combination of both directed evolution and rational protein designs [1, 25, 26].

Approximately 50–70 % neutral and 30–50 % deleterious amino acid substitutions are introduced by ep-PCR [27, 28], yet only 0.5 % are beneficial [29]. The extensive classification of an amino acid substitution as neutral, beneficial, or deleterious depends on the structural stability of the target protein before such a substitution occurs [13]. This could imply that the structural stability of a protein should be considered before it is engineered. The structural stability of many biomolecules usually depends on various interactions such as hydrophilic and hydrophobic interactions [30, 31]. By engineering a relatively more hydrophobic core of an enzyme, its structural stability and ultimately the catalytic efficiency could likely be improved. However, not so many reports have linked hydrophobicity to structural stability and catalytic efficiency of an enzyme. Because of the speculation that hydrophobic interactions are among the key forces that stabilize the structure of many enzymes [31], our goal in this study is not only to improve the enzymatic properties of PpADI under physiological conditions but also to study the relationship between the hydrophobicity, structural stability, and enzymatic properties of PpADI through our hydrophobic mutagenesis concept.

Materials and Methods

Strains and Culture Conditions

In this study, *Escherichia coli* JM109 was used as the cloning host and *E. coli* BL21 (DE3) was used as the expression host as previously described [1]. PpADI mutant M314 generated previously [1] was used in this study.

Reagents and Materials

PrimeSTAR® HS DNA Polymerase was purchased from Takara Biotechnology (Dalian). *DpnI* used was purchased from New England Biolabs. Bradford reagent and plasmid DNA purification kits were purchased from Sangon Biotech (Shanghai, China). All enzymes and kits were used according to the manufacturers' instructions. The acid ferric solution used in the activity assay consisted of 160 mL of 95 % H₂SO₄, 70 mL of 85 % H₃PO₄, and 0.1 g FeCl₃ in a final volume of 1 L. The diacetylmonoxime thiosemicarbazide solution (DAM–TSC) used consisted of 1 % (w/v) diacetyl monoxime and 0.03 % (w/v) thiosemicarbazide. All solutions and reagents used were made as previously described [1, 32]. All other chemicals were either of analytical or higher grades from Sinochem (Shanghai, China).

Site-Directed Mutagenesis

Point mutations were introduced into various PpADI variants using whole plasmids (pET24a-ADI) as templates according to the published overlap extension site-directed mutagenesis (SDM) method [33]. Primers used in this study are shown in Table 1. Total PCR reaction volume was 20 µL and consisted of 10 ng template pET24a-ADI, 1×Primestar buffer, 0.3 µM of each primer, 0.2 mM dNTP mix, and 2.5 units of PrimeSTAR HS DNA polymerase. The thermal cycling conditions were as follows: 95 °C for 5 min; followed by 25 cycles of 95 °C for 20 s, 60 °C for 10 s, and 68 °C for 7 min; and final incubation at 68 °C for 5 min.

Table 1 Oligonucleotides used in this study

Primer name	Target site	Oligonucleotide sequence (5' to 3')
D38H-F	38	CCGAGCAACTGCC <u>ACG</u> GAGCTGCTGTTCGACGATG
D38H-R	38	CATCGTCCAACAGCAGCTC <u>GTGG</u> CAGTTGCTCCGG
E296K-F	296	GTCACGGTTTTCCCG <u>AAA</u> GTGGTGCGCGAGAT
E296K-R	296	ATCTCGCGCACCACTTT <u>CGGG</u> AAAACCGTGAC
S245D-F	245	ATGGGTGAGCGCAC <u>CGAT</u> CGCCAGGCCATC
S245D-R	245	GATGGCCTGGCG <u>ATCG</u> GTGCGCTCACCCAT
SSM-Q162-F	162	GCTGCCAACACCC <u>NNK</u> TTCACCCGCGACAC
SSM-Q162-R	162	GTGTGCGGGGTGA <u>AMN</u> NGGTGTTGGGCAGC
SSM-S245-F	245	ATGGGTGAGCGCAC <u>NNK</u> CGCCAGGCCATC
SSM-S245-R	245	GATGGCCTGGCG <u>MNN</u> GGTGCGCTCACCCAT
ADI-R243L-F	243	ATGGGTGAG <u>CTC</u> ACCTCGC
ADI-R243L-R	243	GCGAGGT <u>GAG</u> CTCACCCAT
243-SSM-F	243	ATGGGTGAG <u>NNK</u> ACCTCGC
243-SSM-R	243	GCGAGGT <u>MNN</u> CTCACCCAT
ADI-R243I-F	243	GGCATGGGTGAG <u>ATA</u> ACCTC
ADI-R243I-R	243	GAGGT <u>TAT</u> CTCACCCATGCC
ADI-R243V-F	243	ATGGGTGAGGT <u>GAC</u> CTCGC
ADI-R243V-R	243	GCGAGGT <u>CAC</u> CTCACCCAT
A276W-F	276	CGAAGTCCC <u>GTGCG</u> TGGATGC
A276W-R	276	GCAT <u>CCAC</u> GCACGGGACTTCG

Subsequently, the PCR product was treated with *Dpn* I to digest the parent plasmid prior to transformation into *E. coli* JM109 and later into *E. coli* BL21 for protein expression.

Expression and Purification of PpADI Variants

In this study, all PpADI mutants were cultured and purified as previously described [1]. Briefly, the recombinant *E. coli* strains were cultured overnight at 37 °C in liquid Luria Bertani (LB) medium supplemented with kanamycin. The overnight culture was then inoculated into fresh LB medium, and isopropyl- β -D-thiogalactopyranoside (IPTG) was added for induction when optical density at 600 nm (OD_{600}) reached 0.6. The culture was incubated for 4 h at 120 rpm and 30 °C. The cells were then harvested by centrifugation and suspended in 20 mM phosphate buffer (PBS, pH 7.0). Subsequently, crude enzyme extracts were purified by ion exchange chromatography on a HiPrep DEAE FF 16/10 column (GE Healthcare, Sweden). The protein samples from DEAE column were then purified by gel filtration chromatography using Superdex 200 10/300 gel filtration column (GE Healthcare, Sweden). All purification procedures were conducted as previously described [1]. All mutants generated were verified by DNA sequencing. Upon expression in *E. coli* BL21 (DE3), no significant differences in expression levels were observed for various PpADI mutants (data not shown). After sodium dodecyl sulfate polyacrylamide gel electrophoresis (SDS-PAGE), the estimated molecular mass of PpADI from these mutants was approximately 49 kDa which was similar to that of wild type (WT) PpADI [34].

Activity Assay and Characterization of PpADI Variants

The specific activity assay (citrulline detection assay) and kinetic characterizations were performed as previously described [10]. Briefly, the activity assay involves incubating purified ADI with L-arginine (suspended in 0.5 M sodium phosphate buffer, pH 7.4) for 30 min at 37 °C. The mixture was then heated at 100 °C to terminate the reaction after which acid-ferric solution and DAM-TSC solution were added. Finally, the mixture was boiled at 100 °C for 10 min and its optical density at 530 nm was measured. The ADI concentration of each variant was determined using Bradford reagent (Beyotime, China) with bovine serum albumin (BSA) as standard. Kinetic characterization of various PpADI variants was conducted by measuring the amount of citrulline produced at various concentration of arginine (1–10 mM, suspended in 0.5 M sodium phosphate buffer, pH 7.4), from which Lineweaver-Burk plots were generated and kinetic determined.

Molecular Modeling of PpADI Variants

In this study, DNAMAN software (version 5.2.2; Lynnon Biosoft) and PYMOL software (DeLano Scientific LLC) were utilized to construct molecular models of PpADI variants. Since ADI from *Pseudomonas aeruginosa* (PaADI) shares the highest sequence identity (84.2 %) with PpADI, the crystal structures of PaADI (without substrate: 1RXX; with bound substrate: 2A9G) [35] generated by SWISS-MODEL (www.expasy.ch/tools) [36] were used for structural prediction and molecular modeling. Site saturation mutagenesis (SSM) was conducted as previously described [1, 37]. Molecular docking was performed using Autodock 4.2 software [38] with a genetic algorithm.

Thermal and pH Properties of PpADI Variants

Thermal Properties

Various thermal parameters such as optimum temperature (T°), half inactivation temperature (T_{50}), kinetic thermal stability (T_{50}^{15}), and half-life ($t_{1/2}$) have been used to study the thermal profile of various enzymes [26, 32, 39]. T_{50} is the temperature at which 50 % of residual activity was measured than that at optimum temperature. In the present study, T° of PpADI mutants (M314, M13, and M13-9) was determined at various temperatures (30–90 °C) at pH7.4. T_{50} values were estimated from the data obtained.

The kinetic thermal stability (T_{50}^{15}) of an enzyme is the temperature that reduces the initial activity by 50 % in 15 min. The kinetic thermal stability (T_{50}^{15}) of PpADI mutants (M314, M13, M13-9) was also determined. Briefly, 25 μ L of purified enzyme samples (0.1–0.3 mg/mL) suspended in 0.5 M sodium phosphate buffer (pH 7.4) was incubated at various temperatures (25–85 °C) for 15 min. The residual activities were expressed as percentages relative to the activities measured at physiological conditions (37 °C, pH 7.4).

Thermostability analysis ($t_{1/2}$) of PpADI mutants (M314, M13, and M13-9) was performed according to the following method. Briefly, 25 μ L of purified enzyme samples (0.1–0.3 mg/mL) was incubated at 50 or 60 °C prior to activity assay. Residual activity was determined at regular time intervals using the initial activity of each enzyme (without incubation at 50 or 60 °C) as 100 %.

pH Profile

The effect of pH on activity of PpADI variants (M314, M13, and M13-9) was investigated at different pHs (3.0–10.5) as previously described [1]. Relative activities of PpADIs were expressed as percentages relative to that measured at their optimum pHs.

All the activities were measured following the procedure described in section “Activity Assay and Characterization of PpADI Variants” except that different temperatures and pHs were employed as indicated above.

Results

Construction of PpADI Variants

With M314 (A128T/H404R/I410L) as the template, two excellent substitutions (D38H and E296K) identified previously [37] were incorporated to generate variant M13 (D38H/A128T/E296K/H404R/I410L). Improved ADI variant M13 was used as a parent in this study. Based on the sequence alignment and structural model analysis, candidate residues including Ser 245, Arg 243, Ala 276, and Gln162 were selected as hot spots for mutational spiking in further studies. Residue Ser 245 is located approximately 13.85 Å from the substrate (pdb entry 2A9G) and is not highly conserved among various ADIs (Fig. 1). Located in the terminal loop (Fig. 2a), position 245 is occupied by Ser in PpADI, PaADI, and LIADI, while Ser is replaced by Asp at 245 in MaADI (Fig. 1). SSM at position 245 was performed with M13 as a template. Around 350 variants with positive activity were screened, from which a mutant carrying S245D substitution exhibited the highest activity (Table 2).

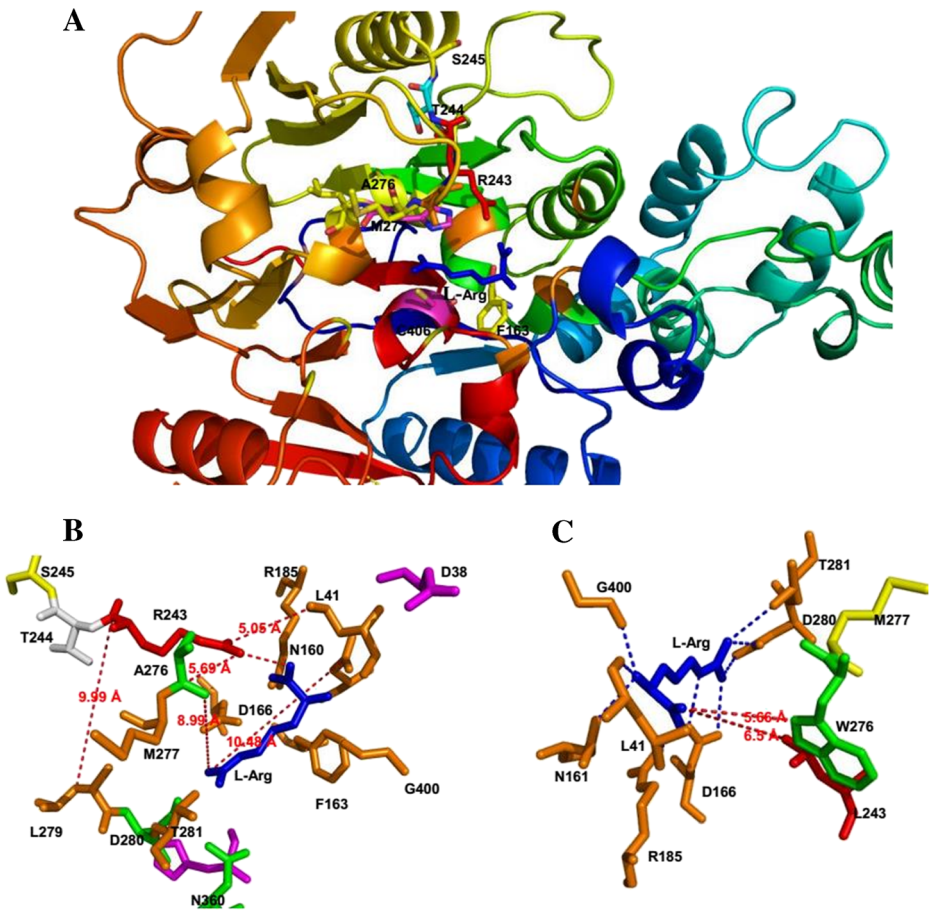


Fig. 2 **a** Molecular model of ADI displaying location of R243 (red) and S245 (yellow) in the terminal loop as well as key residues surrounding the substrate L-arginine (blue); **b** positions of R243 (red) and other first plus and second shell residues; **c** inter-atomic distances of W276 (green), L243 (red), and other key residues (orange) from substrate (blue) (Color figure online)

Table 2 Specific activity and kinetic characterization of selected PpADI variants

Variants	pH 7.0	pH 7.4			
	Specific activity (U/mg) ^a	Specific activity (U/mg) ^a	K_m (mM)	k_{cat} (s ⁻¹)	k_{cat}/K_m (s ⁻¹ mM ⁻¹)
M314 (A128T/H404/I410L)	17.7±0.18	9.02±0.17	0.65	27.20	41.85
M13 (M314+D38H/E298K)	22.00±0.98	15.23±0.04	0.52	21.27	40.93
M13-2 (M13+S245D)	30.08±1.54	21.19±1.03	0.59	22.40	37.97
M13-5 (M13+R243L)	34.23±0.12	31.20±0.07	0.16	30.25	189.06
M13-9 (M13+A276W)	28.10±0.38	18.68±0.65	0.62	20.94	33.77

^a Values are averages±standard deviation

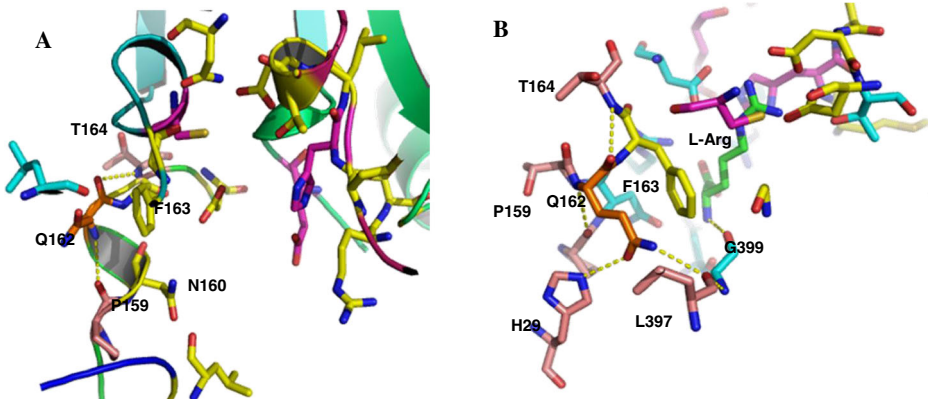


Fig. 3 Molecular model displaying polar hydrogen bonds of Q162 before (a) and after (b) substrate (L-Arg) binding

Influence of Position 162 on the Soluble Expression of PpADI

Mutants carrying Q162S, Q162T, and Q162G mutations displayed measurable activity while all other mutants in the SSM library showed a complete loss in activity. Interestingly, the total protein concentration of the crude cell extracts from M13+Q162S and M13+Q162T increased by 24.16 and 20.81 %, respectively, in comparison with that of M13 (1.49 mg/mL). For mutant M13+Q162G, the specificity activity was lower than that for M13 while its protein concentration (1.52 mg/mL) was slightly higher than that of M13 (Table 3). SDS-PAGE analysis confirmed that the soluble expression of PpADI was observably improved by mutations Q162S and Q162T (Fig. 4). Our results indicate that PpADI's soluble expression levels could be increased when residue Gln 162 is substituted by amino acids with smaller polar R group, such as serine and threonine.

Hydrophobic Mutagenesis and Construction of M13-9

The side chains of hydrophobic amino acid residues tend to be buried in a protein's interior, away from its water microenvironment [30, 31]. Moreover, most enzymes applied in aqueous media have relatively hydrophobic cores and hydrophilic surfaces [30]. In WT PpADI, position 276 is occupied by alanine, which is also located in the terminal loop adjacent one of the catalytic triad residues (Met 277) and is approximately 8.99 Å from the substrate

Table 3 Characterization of various mutants at residue 162 at pH 7.4

Mutants	Activity (U/mL) ^a	Protein concentration (mg/mL) ^a	Specific activity (U/mg) ^a
M13 (M314+D38H/E298K)	13.03±0.03	1.49±0.04	8.75±0.05
M13+Q162S	15.78±0.24	1.85±0.01	8.53±0.06
M13+Q162T	15.04±0.13	1.80±0.07	8.34±0.28
M13+Q162G	10.98±0.03	1.52±0.02	7.20±0.11

^a Values are averages±standard deviation obtained using crude enzyme extracts

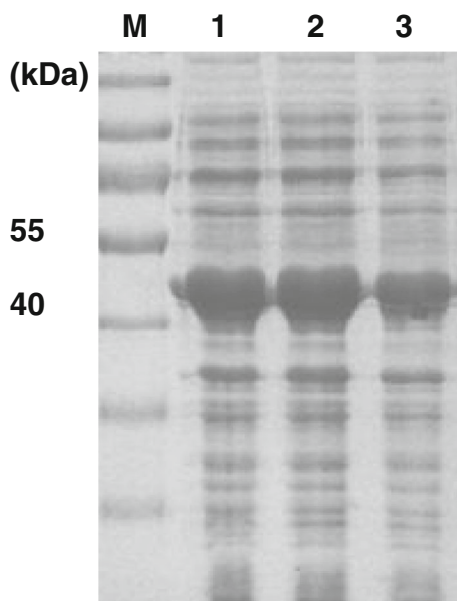


Fig. 4 SDS-PAGE of crude cell extract of PpADI variants. Lanes: *M*, marker; *1*, M13+Q162S; *2*, M13+Q162T; and *3*, M13. Equal volumes of crude cell extracts were loaded on the gel. Each ADI subunit is estimated to have a molecular weight of approximately 49.0 kDa

(Fig. 2b). Since Ala has a highly nonreactive aliphatic side chain [30], it is therefore speculated that a mutation at Ala 276 might not greatly affect the enzymatic activity of PpADI. Furthermore, substitution of a more hydrophobic amino acid for alanine would certainly increase the hydrophobicity in this region which could possibly increase the structural stability of the enzyme. At pH 7.0, Phe, Ile, Trp, Leu, and Val have higher hydrophobicity than Ala [41]. Despite the possible occurrence of steric hindrance, the aromatic side chains of Trp and Phe usually do not affect an enzyme's catalytic function when present in the catalytic regions of an enzyme [30]. Since hydrophobic interaction often occurs within a 1–8-Å range, a relatively larger and more hydrophobic amino acid is preferable to intensify hydrophobic interactions at this position. Trp was therefore selected due to its high hydrophobicity and relatively larger size than Phe. After the substitution, Trp 276 is approximately 5.66 Å (green) from the substrate (blue) (Fig. 2c), whereas Ala 276 is around 8.99 Å from the substrate (Fig. 2b). Although Trp might not be the best substitute for Ala, mutation A276W produced an interesting outcome in M13-9 (M13+A276W). The specific activity of M13-9 (18.68 U/mg) was higher than that of M13 (15.23 U/mg) but lower than that of M13-5 (31.2 U/mg) (Table 2).

Activity and Kinetics of PpADI Variants

The influence of various mutations on the PpADI activity (at pH 7.0 and 7.4) was investigated and tabulated in Table 2. All mutants exhibited noticeable increments in activity at pH 7.0 and 7.4. In comparison with M314 (17.7 U/mg), M13, M13-2, M13-5, and M13-9 showed significant enhanced specific activity at pH 7.0. The specific activities of M13, M13-2, M13-5, and M13-9 were 22.00, 30.08, 34.24, and 28.10 U/mg, approximately 1.24-, 1.70-,

1.93-, and 1.59-fold that of M314, respectively. However, all mutants showed 8.9–33.5 % reduction in specific activities at pH 7.4 than those at pH 7.0. M13-5 demonstrated the highest specific activity of 31.20 U/mg at pH 7.4 among all variants. The kinetics parameters of PpADI mutants at pH 7.4 were also investigated. M13-5 exhibited a drastically dropped K_m value from 0.52 to 0.16 mmol/L, representing a 3.3-fold decrease than that of M13. As expected, a stunning k_{cat}/K_m value of 189.06 s⁻¹ mM⁻¹ was obtained for M13-5. Based on the molecular docking study (using Autodock 4.2 software), the substrate binding energy for M13, M13-5, and M13-9 was estimated. M13 has a binding energy of approximately -3.71 kcal/mol, in comparison with -4.27 and -6.26 kcal/mol for M13-5 and M13-9, indicating that both substitutes R243L and A276W promote the formation of enzyme-substrate complex.

pH Profile of PpADI Variants

The influence of pH on the activity of WT, M314, M13, and M13-9 was also studied (Fig. 5). The optimum pH of all PpADI mutants was around 6.5, slightly enhanced compared with that of WT (pH 6.0). Interestingly, mutant M13-9 displayed tremendous pH stability (retained over 90 % activity over a pH range of 4.5–8.5). However, a drastic reduction in activity of M13-9 was observed beyond this pH range, merely 30 % residual activity was observed at pH 3.5 and 9.0. At pH 7.4, M13 and M314 retained approximately 63 and 48 % of their highest activity (at pH 6.5), while no residual activity was detected at pH 3.5 and 8.5.

Thermal Properties of PpADI Variants

In this study, the thermal properties of PpADI variants were determined (Table 4). Similar to pH stability study, M13-9 displayed the highest thermostability among all variants tested. The optimum temperature (T^o) of mutants M314, M13, and M13-9 were 32, 45, and 62 °C,

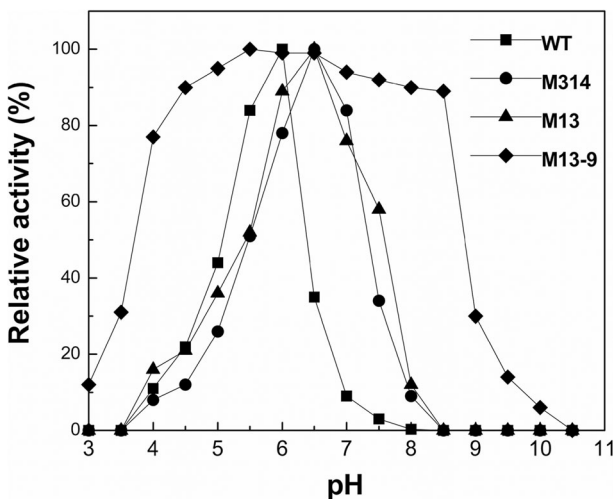


Fig. 5 Effect of pH on activity of PpADI WT, M314, M13, and M13-9; activity was expressed as percentages relative that measured at optimum pH of each variant

Table 4 Thermal characterization of M314, M13, and M13-9

PpADI variants	Specific activity (U/mg) ^a	T^o (°C)	Specific activity at T^o (U/mg) ^b	T_{50} (°C) ^d	T_{50}^{15} (°C) ^e	$t_{1/2}$ [50 °C] (h) ^f	$t_{1/2}$ [60 °C] (min)
M314	9.02	32	9.92	52	55	3.8	2.5
M13	15.23	45	16.75	60	56	6.1	4
M13-9	18.68	62	93.40	78	58	6.6	17.5

^a Specific activity is determined at 37 °C with 10 mM L-arginine suspended in phosphate buffer (pH 7.4)

^b Specific activity is determined at T^o with 10 mM L-arginine suspended in phosphate buffer (pH 7.4)

^c T^o is the optimum temperature

^d T_{50} is the half inactivation temperature at which 50 % of residual activity was measured

^e T_{50}^{15} is the temperature that reduces initial activity by 50 % in 15 min

^f $t_{1/2}$ is half-life time of the enzyme

respectively. At their individual T^o , the specific activity of M13 (16.75 U/mg) and M13-9 (93.4 U/mg) was approximately 1.7- and 9.4-fold that of M314 (9.92 U/mg). Interestingly, the specific activity of M13-9 at 62 °C was approximately fivefold that determined at 37 °C (18.68 U/mg), whereas M314 and M13 showed only 10 % increase in specific activity at their T^o than that determined at 37 °C. Mutants M314, M13, and M13-9 displayed comparable kinetic thermal stability (T_{50}^{15}) values, specifically 55, 56, and 58 °C.

As expected, M13-9 exhibited the highest half-inactivation temperature (T_{50}) and half-life ($t_{1/2}$) values. The T_{50} of M13-9, M13, and M314 was around 78, 60, and 52. At 60 °C, $t_{1/2}$ of M13-9, M13, and M314 was approximately 17.5, 4.0, and 2.5 min, whereas the values were significantly higher at 50 °C (approximately 6.6, 6.1, and 3.8 h) (Fig. 6). At lower temperatures, all mutants displayed considerably higher thermal stability. For instance, the $t_{1/2}$ of M13-9 at 45 °C was approximately 12 h (data not shown).

Discussion

Compared with M13, M13-2 showed a significantly increased specific activity and a similar K_m value at physiological conditions (Table 2). It is not clear why only the S245D substitution in M13-2 led to the observed increment in catalytic function. However, the possibility of Ser 245 and Asp 245 being helix capping groups in PpADI explains their effectiveness in maintaining ADI activity. This is probably why the substitution by any other amino acids at this position via SSM did not lead to improved ADI activity. In addition, the increase in PpADI solubility as a result of the Q162S and 162 T mutations was also not clearly interpreted. This increase in protein expression is expected to boost ADI recovery especially after the two rounds of purification done prior to its characterization and utilization. Shi and coworkers demonstrated that protein engineering is an efficient method for improving soluble expression of heterologous proteins in *E. coli* [42]. The increased expression levels in Q162S and 162 T mutants could be attributed to the improved mRNA stability that resulted in enhanced transcription. The presence of rare codons in coding sequences of heterologous proteins has also been suggested to assist the transcription of such proteins [43]. Whereas it is not completely the case in this study, the observed codons

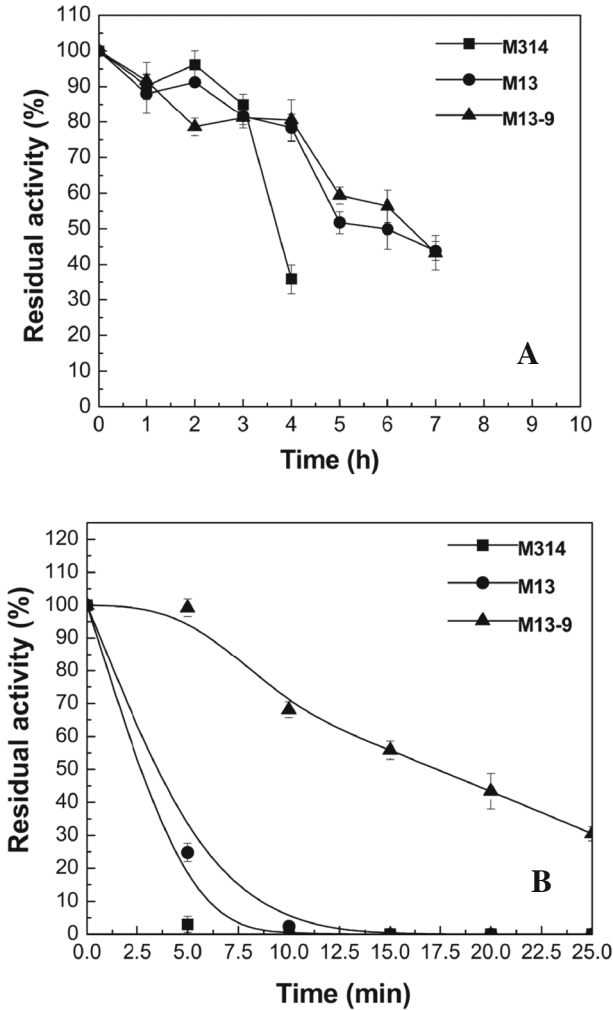


Fig. 6 Thermostability of PpADI at 50 °C (a) and 60 °C (b). Purified enzyme samples were incubated at 50 or 60 °C prior to activity assay. Residual activity was determined at regular time intervals. Data were obtained from three independent experiments

for Ser and Thr in Q162S and Q162T were AGC and ACC which are not rare codons. Therefore, the exact mechanism for the increased soluble expression of PpADI is not completely understood.

Mutant M13-5 exhibited significantly enhanced specific activity and substrate binding affinity, as illustrated by the dramatically reduced K_m value (0.16 mmol/L) and a more favorable free energy of L-arginine binding ($-\Delta G=4.27$ kcal/mol) at physiological conditions. These results indicate that M13-5 could bind the substrate (L-arginine) more readily than M13. Furthermore, substitution of a highly hydrophobic leucine residue for a highly amphipathic arginine at position 243 (R243L) (Fig. 2b, c) in M13-5 resulted in dramatic improvements in both structural stability and substrate

affinity. This presumption is supported by the results from mutant M13-9 (M13+A276W) generated through the hydrophobic mutagenesis approach. M13-9 displayed tremendous pH and thermal stability, suggesting the increase in hydrophobicity around the active site brought about the enhanced structural stability of PpADI.

Protein denaturation from either pH or heat extremities usually results in loss of catalytic function in almost all enzymes. Heat denaturation, for instance, usually affects weak interactions such as hydrogen bonds which ultimately destabilize the native conformation of proteins. Consequently, proteins work well within a specific temperature and pH range beyond which denaturation affects catalytic function [30]. Since the impact of heat on proteins is not easily predicted, obtaining a relatively thermal and pH stable enzyme for a given catalytic role is extremely beneficial. In our study, mutant M13-9 displayed remarkable pH and thermal tolerance. It is presumed that the hydrophobic substitution A276W in M13-9 leads to an increase in structural stability of the active site surrounding, and ultimately higher enzymatic activity. Our results indicate that it is quite possible to enhance the structural stability of a protein through one or several amino acid substitutions by targeted design approaches such as the hydrophobic mutagenesis strategy.

Due to its remarkable thermal stability, it is expected that M13-9 will be highly stable when utilized at physiological conditions. Its pH stability also ensures that the catalytic function would not be severely affected by subsequent modifications for enhanced pharmacokinetic and pharmacodynamic properties as we attempted on PpADI M13-3 in previous study [11], for example, PEGylation and subsequent drug formulation. The kinetic thermal stability profile indicates that a prior heat activation (25–50 °C) or incubation might be necessary for effective catalysis of PpADI (Fig. 7). The results also suggest that our hydrophobic mutagenesis concept could be a promising approach in designing better PpADI variants. This algorithm could not only prove vital in subsequent PpADI engineering process but also become a basis in the development of related rational design algorithms that could be beneficial to many protein engineers.

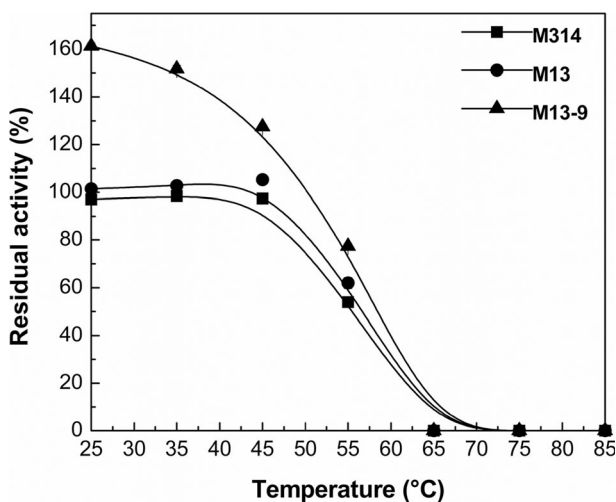


Fig. 7 Kinetic thermal stability profile of M314, M13, and M13-9 PpADI. Purified enzyme samples were incubated at various temperatures for 15 min prior to determination of residual activity relative that measured at 37 °C without heat exposure. Data were obtained from three independent experiments

Conclusion

Taken together, the enzymatic properties of PpADI at physiological conditions were successfully improved by protein engineering based on semi-rational design. Our results suggest that the enhanced hydrophobicity around the catalytic center may result in improved structural stability of an enzyme as well as its catalytic function. This study could provide an experimental and theoretical rationale for protein engineering of ADI for improved stability and catalytic properties as well as soluble protein expression, and is therefore important for the development of ADI as a novel anti-tumor drug.

Acknowledgments We are grateful to the Natural Science Foundation of China (21276112, 31401634), National Basic Research and Development Program of China (973 Program, 2011CB710800), New Century Excellent Talents in University (NCET-11-0658), the Fundamental Research Funds for the Central Universities (JUSRP51409B), the Program of Introducing Talents of Discipline to Universities (111-2-06), and a project funded by the Priority Academic Program Development of Jiangsu Higher Education Institutions for the financial support of this research.

References

1. Ni, Y., Liu, Y. M., Schwaneberg, U., Zhu, L. L., Li, N., Li, L. F., & Sun, Z. H. (2011). Rapid evolution of arginine deiminase for improved anti-tumor activity. *Applied Microbiology and Biotechnology*, *90*, 193–201.
2. Miyazaki, K., Takaku, H., Umeda, M., Fujita, T., Huang, W. D., Kimura, T., Yamashita, J., & Horio, T. (1990). Potent growth inhibition of human tumor cells in culture by arginine deiminase purified from a culture medium of a *Mycoplasma*-infected cell line. *Cancer Research*, *50*, 4522–4527.
3. Takaku, H., Takase, M., Abe, S. I., Hayashi, H., & Miyazaki, K. (1992). In vivo anti-tumor activity of arginine deiminase purified from *Mycoplasma arginini*. *International Journal of Cancer*, *51*, 244–249.
4. Gong, H., Zölzer, F. G., von Recklinghausen, G., Havers, W., & Schweigerer, L. (2000). Arginine deiminase inhibits proliferation of human leukemia cells more potently than asparaginase by inducing cell cycle arrest and apoptosis. *Leukemia*, *14*, 826–829.
5. Ni, Y., Schwaneberg, U., & Sun, Z. H. (2008). Arginine deiminase, a potential anti-tumor drug. *Cancer Letters*, *261*, 1–11.
6. Ott, A. P., Carvajal, R. D., Taskar, N. P., Jungbluth, A. A., Hoffman, E. W. W., Bomalaski, B. W., Venhaus, J. S., Pan, R., Old, L., Pavlick, L. J., Pavlick, A. C., & Wolchok, J. D. (2013). Phase I/II study of pegylated arginine deiminase (ADI-PEG 20) in patients with advanced melanoma. *Investigational New Drugs*, *31*, 425–434.
7. Yang, T., Lu, S. T., Chao, Y., Sheen, I. S., Lin, C. C., Wang, T. E., Chen, S. C., Wang, J. H., Liao, L. Y., Thomson, J. A., Wang-Peng, J., Chen, P. J., & Chen, L. T. (2010). A randomised phase II study of pegylate d arginine deiminase (ADI-PEG 20) in Asian advanced hepatocellular carcinoma patients. *British Journal of Cancer*, *103*, 954–960.
8. Izzo, F., Marra, P., Beneduce, G., Castello, G., Vallone, P., Rosa, V. D., Cremona, F., Ensor, C. M., Holtsberg, F. W., Bomalaski, J. S., Clark, M. A., Ng, C., & Curley, S. A. (2004). Pegylated arginine deiminase treatment of patients with unresectable hepatocellular carcinoma: results from phase I/II studies. *Journal of Clinical Oncology*, *22*, 1815–1822.
9. Shen, L. J., & Shen, W. C. (2006). Drug evaluation: ADI-PEG-20-a PEGylated arginine deiminase for arginine-auxotrophic cancers. *Current Opinion in Molecular Therapeutics*, *8*, 240–248.
10. Liu, Y. M., Sun, Z. H., Ni, Y., Zheng, P., Liu, Y. P., & Meng, F. J. (2008). Isolation and identification of an arginine deiminase producing strain *Pseudomonas plecoglossicida* CGMCC2039. *World Journal of Microbiology and Biotechnology*, *24*, 2213–2219.
11. Zhang, L., Liu, M., Jamil, S., Han, R., Xu, G., & Ni, Y. (2015). PEGylation and pharmacological characterization of a potential anti-tumor drug, an engineered arginine deiminase originated from *Pseudomonas plecoglossicida*. *Cancer Letters*, *357*, 346–354.
12. Stemmer, W. P. (1994). Rapid evolution of a protein in vitro by DNA shuffling. *Nature*, *370*, 389–391.

13. Bloom, J. D., & Arnold, F. H. (2009). In the light of directed evolution: Pathways of adaptive protein evolution. *Proceedings of the National Academy of Sciences of the United States of America*, *106*, 9995–10000.
14. Wang, Q., Du, W., Weng, X. Y., Liu, M. Q., Wang, J. K., & Liu, J. X. (2015). Recombination of thermo-alkalstable, high xylooligosaccharides producing endo-xylanase from *Thermobifida fusca* and expression in *Pichia pastoris*. *Applied Biochemistry and Biotechnology*, *175*, 1318–1329.
15. Johannes, T. W., & Zhao, H. (2006). Directed evolution of enzymes and biosynthetic pathways. *Current Opinion in Microbiology*, *9*, 261–267.
16. Zhao, H., & Arnold, F. H. (1997). Combinatorial protein design: strategies for screening protein libraries. *Current Opinion in Structural Biology*, *7*, 480–485.
17. Turner, N. J. (2009). Directed evolution drives the next generation of biocatalysts. *Nature Chemical Biology*, *5*, 567–574.
18. Xu, W., Shao, R., Wang, Z., & Yan, X. (2015). Improving the neutral Phytase activity from *Bacillus amyloliquefaciens* DSM 1061 by site-directed mutagenesis. *Applied Biochemistry and Biotechnology*, *175*, 3184–3194.
19. Bommarius, A. S., Broering, J. M., Chaparro, R. J. F., & Polizzi, K. M. (2006). High throughput screening for enhanced protein stability. *Current Opinion in Biotechnology*, *17*, 606–610.
20. Lutz, S. (2010). Beyond directed evolution—semi-rational protein engineering and design. *Current Opinion in Biotechnology*, *21*, 734–743.
21. Zhang, D., Zhu, F., Fan, W., Tao, R., Yu, H., Yang, Y., Jiang, W., & Yang, S. (2011). Gradually accumulating beneficial mutations to improve the thermostability of N-carbamoyl-D-amino acid amidohydrolase by step-wise evolution. *Applied Microbiology and Biotechnology*, *90*, 1361–1371.
22. Tian, Y. S., Peng, R., Xu, J., Zhao, W., Gao, F., Fu, X. Y., Xiong, A. S., & Yao, Q. H. (2011). Semi-rational site-directed mutagenesis of phyl1s from *Aspergillus niger* 113 at two residue to improve its phytase activity. *Molecular Biology Reports*, *38*, 977–982.
23. Dror, A., & Fishman, A. (2012). Engineering non-heme mono- and dioxygenases for biocatalysis. *Computational and Structural Biotechnology Journal*, *2*, 1–12.
24. Li, X. J., Zheng, R. C., Ma, H. Y., & Zheng, Y. G. (2014). Engineering of *Thermomyces lanuginosus* lipase Lip: creation of novel biocatalyst for efficient biosynthesis of chiral intermediate of Pregabalin. *Applied Microbiology and Biotechnology*, *98*, 2473–2483.
25. Cheng, F., Zhu, L. L., Lue, H. Q., Bernhagen, J., & Schwaneberg, U. (2015). Directed arginine deiminase evolution for efficient inhibition of arginine-auxotrophic melanomas. *Applied Microbiology and Biotechnology*, *99*, 1237–1247.
26. Zhu, L. L., Cheng, F., Piatkowski, V., & Schwaneberg, U. (2014). Protein engineering of the antitumor enzyme PpADI for improved thermal resistance. *ChemBioChem*, *15*, 276–283.
27. Shafikhani, S., Siegel, R. A., Ferrari, E., & Schellenberger, V. (1997). Generation of large libraries of random mutants in *Bacillus subtilis* by PCR-based plasmid multimerization. *BioTechniques*, *23*, 304–310.
28. Drummond, D. A., Silberg, J. J., Meyer, M. M., Wilke, C. O., & Arnold, F. H. (2005). On the conservative nature of intragenic recombination. *Proceedings of the National Academy of Sciences of the United States of America*, *102*, 5380–5385.
29. Bloom, J. D., Labthavikul, S. T., Otey, C. R., & Arnold, F. H. (2006). Protein stability promotes evolvability. *Proceedings of the National Academy of Sciences of the United States of America*, *103*, 5869–5874.
30. Nelson, D. L., & Cox, M. M. (2004). *Lehninger principles of biochemistry*, 4th Edition. Freeman, W.H. & Company.
31. Gong, Y., Xu, G. G., Zheng, W. G., Li, X. C., & Xu, H. J. (2014). A thermostable variant of *Bacillus subtilis* esterase: characterization and application for resolving dl-methyl acetate. *Journal of Molecular Catalysis B: Enzymatic*, *109*, 1–8.
32. Archibald, R. M. (1944). Determination of citrulline and allantoin and demonstration of citrulline in blood plasma. *Journal of Biological Chemistry*, *156*, 121–142.
33. Wang, W., & Malcolm, B. A. (2002). Two-stage polymerase chain reaction protocol allowing introduction of multiple mutations, deletions and insertions using QuikChange™ site-directed mutagenesis. *Methods in Molecular Biology*, *182*, 37–43.
34. Ni, Y., Li, Z. W., Sun, Z. H., Zheng, P., Liu, Y. M., Zhu, L. L., & Schwaneberg, U. (2009). Expression of arginine deiminase from *Pseudomonas plecoglossicida* CGMCC2039 in *Escherichia coli* and its anti-tumor activity. *Current Microbiology*, *58*, 593–598.
35. Galkin, A., Kulakova, L., Sarikaya, E., Lim, K., Howard, A., & Herzberg, O. (2004). Structural insight into arginine degradation by arginine deiminase, an antibacterial and parasite drug target. *Journal of Biological Chemistry*, *279*, 14001–14008.
36. Schwede, T., Kopp, J., Guex, N., & Peitsch, M. C. (2003). SWISS-MODEL: an automated protein homology-modeling server. *Nucleic Acids Research*, *31*, 3381–3385.

37. Zhu, L. L., Verma, R., Roccatano, D., Ni, Y., Sun, Z. H., & Schwaneberg, U. (2010). A potential antitumor drug (Arginine Deiminase) reengineered for efficient operation under physiological conditions. *ChemBioChem*, *11*, 2294–2301.
38. Morris, G. M., Huey, R., Lindstrom, W., Sanner, M. F., Belew, R. K., Goodsell, D. S., & Olson, A. J. (2009). AutoDock4 and AutoDockTools4: automated docking with selective receptor flexibility. *Journal of Computational Chemistry*, *30*, 2785–2791.
39. Ushasree, M. V., Vidya, J., & Pandey, A. (2015). Replacement P212H altered the pH–temperature profile of phytase from *Aspergillus niger* NII 08121. *Applied Biochemistry and Biotechnology*, *175*, 3084–3092.
40. Goldsmith, M., & Tawfik, D. S. (2013). Enzyme engineering by targeted libraries. In E. Amy (Ed.), *Keating, methods in enzymology* (pp. 256–27). Burlington academic press Volume 523.
41. Monera, O. D., Sereda, T. J., Zhou, N. E., Kay, C. M., & Hodges, R. S. (1995). Relationship of side chain hydrophobicity and α -helical propensity on the stability of the single-stranded amphipathic α -helix. *Journal of Peptide Science*, *1*, 319–329.
42. Shi, Y., Yu, H., Sun, X., Tian, Z., & Shen, Z. (2004). Cloning of the nitrile hydratase gene from *Nocardia* sp. in *Escherichia coli* and *Pichia pastoris* and its functional expression using site-directed mutagenesis. *Enzyme and Microbial Technology*, *35*, 557–562.
43. Chevance, F. F. V., Le Guyon, S., & Hughes, K. T. (2014). The effects of codon context on in vivo translation speed. *PLoS Genetics*, *10*(6), e1004392. doi:10.1371/journal.pgen.1004392.